Kaolin Clay Reinforced with a Granular Column Containing Crushed Waste Glass or Traditional Construction Sands

1. Danish Kazmi (corresponding author)

    Affiliation
    Geotechnical Engineering Centre, School of Civil Engineering, The University of Queensland, Brisbane, QLD 4072, Australia
    Positions
    Research Scholar
    Email address
    d.kazmi@uq.net.au

2. Mehdi Serati

    Affiliation
    Geotechnical Engineering Centre, School of Civil Engineering, The University of Queensland, Brisbane, QLD 4072, Australia
    Position
    Lecturer
    Deputy Manager, Large Open Pit Project (www.lopproject.com)
    Email address
    m.serati@uq.edu.au

3. David J. Williams

    Affiliation
    Geotechnical Engineering Centre, School of Civil Engineering, The University of Queensland, Brisbane, QLD 4072, Australia
    Position
    Professor of Geotechnical Engineering
    Director, Geotechnical Engineering Centre
    Manager, Large Open Pit Project (www.lopproject.com)
    MWT 2020 Conference Chair
    Email address
    d.williams@uq.edu.au

4. Sebastian Quintero Olaya

    Affiliation
    Geotechnical Engineering Centre, School of Civil Engineering, The University of Queensland, Brisbane, QLD 4072, Australia
    Position
    Senior Research Officer
    Email address
    s.quintero@uq.edu.au

5. Sadaf Qasim

    Affiliation
    Department of Civil Engineering, NED University of Engineering and Technology, Karachi, 75270, Pakistan
    Position
    Associate Professor
    Email address
    erum@neduet.edu.pk

6. Yi Pik Cheng

   Affiliation
   Department of Civil, Environmental and Geomatic Engineering, University College London, London, WC1E 6BT, United Kingdom
   Position
   Senior Lecturer
   Email address
   yi.cheng@ucl.ac.uk

7. J. Antonio H. Carraro

   Affiliation
   Department of Civil and Environmental Engineering, Imperial College London, London, SW7 2AZ, United Kingdom
   Position
   Senior Lecturer in Experimental Geotechnical Engineering
   Email address
   antonio.carraro@imperial.ac.uk

Abstract

Installation of granular columns is a cost-effective and versatile *in situ* technique to improve the shear strength, settlement, and drainage behaviour of weak soils. It involves backfilling vertical boreholes in the ground with granular materials stiffer than the native soil, such as stone or compacted sand. However, the massive use and overexploitation of sand and natural aggregates have depleted their reserves in recent decades, causing damage to the environment, creating sand shortages and skyrocketing their price. Hence, it is essential to develop a sustainable alternative to natural aggregates to construct granular columns. The ever-increasing stockpiles of waste glass could be a potential replacement for natural sand in several geotechnical construction applications, noting that both materials have a similar chemical composition. Using crushed waste glass (CWG) as an alternative to traditional natural and manufactured (quarried) sands in granular columns could offer a multi-pronged benefit by recycling non-biodegradable waste (glass) and by conserving a depleting natural resource (sand). Using a large direct shear (LDS) machine, this study investigated the shear strength behaviour of kaolin (to represent a typical weak soil) reinforced with a central granular column. Three different materials were separately used to backfill the column, including natural sand (NS), manufactured sand (MS) and CWG. The results revealed that the geocomposites containing the CWG

80   column have the highest peak friction angle and relatively greater shear strength under high normal

81   stresses, favouring the potential use of CWG as a green alternative to traditional sands in backfilling

82   granular columns, ultimately supporting resource conservation, waste recycling and the paradigm

83   shift towards a circular economy.

84   **Keywords**

85   Granular columns; natural aggregates; crushed waste glass; large direct shear machine; shear

86   strength; geocomposites; circular economy

87
88
89
90
91
92
93
94
95
96
97
98
99
100
101
102
103
104
105
106
107
108
109
110
111
112
113
114
115
116
117
118
119
120
121
122

Introduction

As cities grow, the need to develop low-lying and coastal areas inevitably increase. Low-lying lands are often overlain by soft or loose soils, which are highly compressible and typically marked by low shear strength Malarvizhi (2007), requiring ground improvement before the foundations for new infrastructure could be constructed (Alfaro et al., 1994). Similar challenges are sometimes encountered for inland sand deposits due to water fluctuations in the soil caused by weather changes (Sivakumar et al., 2014). Poor ground properties could be detrimental to infrastructures. For example, the annual damage caused by expansive soils to civil engineering structures is around $1,000 million in the USA, $150 million in the UK and at least $4 million in South Africa (Gourley et al., 1993). The growing land prices and the limited availability of suitable construction sites encourage the need for ground improvement (Babu et al., 2013). Several ground improvement techniques have been developed to improve the geotechnical characteristics of weak *in situ* soils, such as bearing capacity and settlement (Andreou et al., 2008).

Of all the ground improvement techniques available, granular columns, also known as sand or stone columns, granular piles or granular inclusions, are considered one of the most cost-effective and versatile *in situ* ground improvement techniques whose concept was first applied in France in 1830 (Babu et al., 2013). In this technique, vertical boreholes are formed in the soil that are filled upwards with compacted granular backfill such as sand or stone (Castro, 2017). They can be used to improve several types of soil, from soft clays to loose sands, making them one of the preferred ground improvement techniques (Abhishek et al., 2016). They also serve as vertical drains and dissipate excess pore water pressure due to loading by providing a shorter drainage path of higher permeability, thereby increasing the consolidation rate and reducing the time required for post-construction ultimate settlements (Abhishek et al., 2016; McCabe et al., 2007). Another key benefit of granular columns is the densification of the *in situ* soil surrounding the columns, which enhances the compaction characteristics of the *in situ* soil (Ranjan, 1989). Moreover, granular columns could

148   effectively mitigate potential liquefaction or softening of susceptible soils through reinforcement,

149   drainage and densification (Abhishek et al., 2016).

150   According to Sivakumar et al. (2004), a granular column develops end-bearing pressure and shear

151   stresses when loaded vertically, causing the column to expand laterally and mobilise lateral support

152   from the surrounding soil. This increase in lateral stress consolidates the surrounding clay once the

153   excess pore water pressure dissipates and causes further bulging in the column. This process continues

154   until equilibrium is achieved at the boundary between the column and the surrounding clay. As a

155   result, the column and the surrounding clay act as a composite with a higher stiffness than the original

156   soil (Mohapatra et al., 2014). The net result is that the entire site where the columns are installed then

157   displays higher strength, improved bearing capacity and stiffness. Technically, granular columns

158   largely obtain their load capacity from the confinement provided by the surrounding soil by mobilising

159   passive earth pressure (Babu et al., 2013). However, for very soft clays with very low undrained shear

160   strength (<15 kN/m^2), such soils provide insufficient lateral confinement causing the columns to

161   undergo excessive bulging and settlements that reduce the load-carrying capacity and the

162   effectiveness of granular columns (Murugesan & Rajagopal, 2007).

163   Granular columns are mostly installed using the vibro-flotation technique, whose typical installation

164   process is schematically shown in Figure 1. A vibroflot (or vibrating poker) is inserted into the ground

165   to create a vertical hole that is incrementally filled with compacted sand or stone (Ranjan, 1989).

166   Vibro-replacement is generally used for clayey soils (Priebe, 1995). Moreover, granular columns are

167   environment-friendly (Hanna et al., 2013; Mehrannia et al., 2018). They release relatively lower

168   greenhouse gas emissions and consume relatively less fuel during their installation (Chawla et al.,

169   2010).

170   Theoretically, the unit cell model is mostly used to analyse granular columns (Castro, 2017). It consists

171   of a single column and its corresponding tributary area transformed into an equivalent circle (influence

172   zone) with the same cross-sectional area (Ng & Tan, 2015). The diameter of a unit cell is equal to d_e =

173   1.05 – 1.13s for triangular and square grids, respectively, where s is the centre-to-centre spacing

174   between columns (Castro, 2017). Several parameters influence the behaviour of soil reinforced with

175   granular columns, including the area replacement ratio, length and diameter of the column, material

176   properties of the column backfill, spacing between the columns and the installation pattern of the

177   columns (Babu et al., 2013; Bergado et al., 1990; Poorooshasb & Meyerhof, 1997; Priebe, 1995).

178   *Literature review*

179   Several studies have examined the geotechnical performance of soil treated with granular columns.

180   Some of these studies compared the shear resistance and load-settlement response of ordinary and

181   geotextile-encased columns (e.g. Mohapatra et al. 2014, Malarvizhi 2007); however, they are not the

182   focus of this study.

183   Canakci et al. (2017) investigated the shear strength (direct shear) and compressibility (oedometer)

184   performance of fibrous peat soil (liquid limit of 119%) reinforced with a sand column. Rounded poorly-

185   graded sand, passing a 2-mm sieve and retained on a 1-mm sieve, was used to construct the column

186   at three different area replacement ratios (11.5%, 25% and 49%). Their study found that installing a

187   sand column improved the peat's compressibility and shear strength behaviour, with compressibility

188   characteristics improving with increase in the area replacement ratio.

189   Similarly, Najjar et al. (2010) examined the mechanical behaviour of normally consolidated clay

190   (kaolin) reinforced with encased and non-encased sand columns. The sand columns comprised poorly

191   graded Ottawa sand with a friction angle of 33° and were installed at a relative density of nearly 44%.

192   A total of 32 isotropically consolidated undrained (CU) triaxial tests was performed on reinforced

193   specimens with area replacement ratios of 7.9% and 17.8%. The study found that the sand columns

194   considerably reduced the generation of excess pore water pressure during undrained loading. It was

195   also noted that increasing the area replacement ratio from 7.9% to 17.5% considerably increased the

196   undrained shear strength of kaolin reinforced with fully-penetrating non-encased sand columns.

197   Aslani et al. (2019) investigated the shear strength behaviour of clay reinforced with granular columns

198   containing gravel (D_{50} = 0.52 mm) or stone (D_{50} = 4.2 mm). Using a large direct shear machine with an

199   area of 305 mm x 305 mm and depth of 152.4 mm, tests were performed on geocomposites containing

200   three different area replacement ratios (13.3%, 17.7% and 24%), different installation patterns (single,

201   square and triangular) and different normal stresses (35 kPa, 55 kPa and 75 kPa). Their study

202   concluded that the shear strength of the geocomposites increased with increasing area replacement

203   ratio in all granular column installation patterns. The study also observed that installing a granular

204   column increased the stiffness of reinforced clay compared to the unreinforced clay.

205   Barmade et al. (2021) investigated the load-settlement behaviour of expansive soil reinforced with

206   stone columns with diameters of 40 mm, 60 mm and 80 mm. Their study concluded that installing

207   stone columns improved the bearing pressure of the reinforced soil, while the columns also increased

208   the drainage of the soil. Hence, the benefits of installing granular columns in weak soils are well-

209   established in the literature, as discussed in the reviewed studies (Babu et al., 2013; Manohar & Patel,

210   2021; Mokhtari & Kalantari, 2012; Najjar, 2013).

211   *Why should the crushed waste glass be considered for use as an alternative to traditional construction*

212   *sands?*

213   Natural aggregates are fundamentally used to create granular columns. However, due to the

214   continued use and heavy reliance of the construction industry, the aggregates (sand and stone)

215   suitable for construction are rapidly depleting globally (Holmstrom & Swan, 1999; Kazmi et al., 2020c;

216   Kazmi et al., 2019a). Studies show that sand and gravel are being mined at a rate greater than their

217   renewal (Bendixen et al., 2019). As a result, the global demand for natural sand and gravel has

218   skyrocketed to almost 50 billion tonnes per year, averaging 18 kg/person/day (UNEP, 2019). Today

219   many countries in the world face an approaching risk of a shortage of aggregates (Langer et al., 2004).

220   Simultaneously, the mining of aggregates and associated activities typically releases a carbon footprint

221   that is harmful to the environment (Bravo et al., 2015; Kazmi et al., 2020b). Thus, there is a growing

222   need to develop a sustainable replacement for natural and manufactured (quarried) sands in

223   construction, including geotechnical applications (Kazmi et al., 2019b). The ever-increasing volumes

224   of waste glass could provide such an alternative (Kazmi et al., 2021). Nearly 10, 15 and 1 million tons

225   of waste glass are stockpiled every year in United States, European Union and Australia, respectively,

226   creating a challenge for their safe and sustainable disposal (Saberian et al., 2019). According to Kazmi

227   et al. (2019a), given the growing quantities of waste glass and diminishing reserves of natural sand,

228   the use of waste glass as an alternative to natural and manufactured (quarried) sand could provide

229   two-pronged benefits of economy and environmental sustainability. In cities, waste glass is typically

230   produced in greater volumes, and quarries are often far from project sites. Using crushed waste glass

231   (CWG) as an alternative geomaterial could be cost-effective due to low material cost, reduced travel

232   distance and shorter transportation time. Simultaneously, as waste glass is non-biodegradable, such

233   utlisation of CWG could promote waste recycling, decrease burden on landfills, reduce greenhouse

234   gas emissions and conserve natural raw materials, ultimately all leading towards a circular economy.

235   *Common safety concerns associated with the use of crushed waste glass*

236   Generally, a common safety concern associated with using CWG is the risk of skin cut due to sharp

237   edges of glass particles (Ali, 2012). However, practical experience suggests that glass particles finer

238   than 19 mm poses no greater cut or penetration risk than an ordinary fractured natural aggregate (Ali,

239   2012). Another common concern about the use of glass is the risk of contracting silicosis, a respiratory

240   disease caused when crystalline silica is inhaled. However, during the glass manufacturing process,

241   the crystalline silica is largely turned into amorphous silica, which does not primarily lead to silicosis

242   (Clean Washington Center, 1996). Moreover, previous studies show that CWG could be a potential

243   replacement for natural sand in several geotechnical construction applications (Wartman et al., 2004;

244   Disfani et al., 2011; Arulrajah et al., 2013). Kazmi et al. (2020a) compared the geotechnical,

245   mineralogical and morphological behaviour of CWG with those of natural sand (NS) and manufactured

246   sand (MS). Their study concluded that CWG has geotechnical behaviour similar to traditional

247　construction sands and could potentially be used as an alternative smart geomaterial in several

248　geotechnical construction applications (Kazmi et al., 2020a).

249　*Use of alternative geomaterials in granular columns*

250　Granular columns offer an ideal opportunity to utilise recycled aggregates as column backfill (Egan &

251　Slocombe, 2010). However, limited research is done on using alternative materials (waste) to backfill

252　granular columns (Ayothiraman & Soumya, 2015). A few researchers observed some favourable

253　behaviour of granular columns backfilled with different alternative materials, including tyre chips,

254　recycled crushed brick, recycled crushed concrete, recycled railway track ballast, incinerator bottom

255　ash aggregate (IBAA) and construction and demolition waste (Alnunu & Nalbantoglu, 2019; Amini,

256　2016; Ayothiraman & Soumya, 2015; Kumar & Sadana, 2012; Serridge, 2004; Serridge & Sarsby, 2009;

257　Shahverdi & Haddad, 2020). However, despite enormous potential, no detailed study has been found

258　to date investigating the use of CWG as backfill in granular columns.

259　To fill this research gap, this study investigates the shear strength behaviour of geocomposites (soil

260　reinforced with a granular column) with a granular column containing CWG and installed in the centre

261　of a weak clayey soil (kaolin). Several reasons led to the selection of kaolin as the weak soil in this

262　study. Firstly, kaolin has relatively low shear strength and often requires some form of treatment or

263　reinforcement to support applied loads. Also, kaolin is readily available commercially, and its

264　information database is extensive due to the large number of studies involving its use (Mishra et al.,

265　2018a; Mishra et al., 2018b; Mishra et al., 2020; Rossato et al., 1992). The novelty of this paper is that

266　it compares the shear strength behaviour of geocomposites containing a CWG column with those

267　containing a column made up of NS or MS, which are traditionally used in sand column construction

268　(Zukri and Nazir, 2018).

269　**Methodology**

270　In this study, a series of large direct shear tests (LDST) on cubical specimens with length, width and

271　height equal to 150 mm were performed to investigate the shear strength behaviour of

272 geocomposites. Each geocomposite comprised of a cubical kaolin clay specimen (bed material) with a

273 vertical granular column installed in its centre. Distinct geocomposites were prepared using columns

274 containing three different types of column backfill. The LDS tests were also performed on kaolin as a

275 control sample to compare its shear strength behaviour with that of column-kaolin geocomposites.

276 Three different materials were separately used to backfill the granular column, including NS, MS or

277 CWG.

278 Table 1 shows the results of the mineralogical analysis performed on NS, MS and CWG using X-ray

279 fluorescence (XRF) spectroscopy, showing that silica (SiO_2) is the dominant mineral in all three

280 materials. Table 2 presents the geotechnical characterisation results of all the test materials, as

281 reported by Kazmi et al. (2021) and Xu et al. (2018), showing that NS and CWG are uniformly graded

282 materials with median particle sizes of 0.29 mm and 1.42 mm, respectively. The median particle size

283 of NS is almost five times smaller than that of CWG. MS, however, is a well-graded sand with a median

284 particle size of 1.55 mm. Figure 3 illustrates the gradation curves of the test materials.

285 The morphological analysis showed that MS has the highest particle angularity, followed by CWG and

286 NS. This implies that NS particles are relatively more rounded than MS and CWG particles. Figure 2

287 shows the optical microscopic images of NS, MS and CWG particles. Also, the permeability tests

288 revealed that CWG has the highest permeability, followed by NS and MS. CWG has the lowest

289 minimum dry density and the largest difference between maximum and minimum dry density values.

290 The critical-state friction angle of CWG increased by almost 11%, from 29.1° under dry conditions to

291 32.4° under saturated conditions.

292 The kaolin used in this study is a highly plastic clay (CH) with a liquid limit and plasticity index of 90%

293 and 55%, respectively. The percentage of material passing the #200 sieve (F_{200}) is 69% for the kaolin.

294 The advanced high-accuracy large direct shear test machine (LDSM), ADS-300, manufactured by Wille

295 Geotechnik in Germany, was used to test the shear strength of all the specimens. The machine is

296 equipped with four linear variable differential transducers (LVDTs) on four corners of the top-loading

297 cap, recording the average settlement value. The testing setup also features a computer with data

298 logging software to precisely record the measurements. The size of all the geocomposites tested was

299 150 mm x 150 mm x 150 mm. A key reason to use the LDSM is that it provides the ability to test

300 relatively large specimens alongside better control over specimen design parameters. This helps in

301 minimising the size effect and modelling the field conditions more accurately. The device also

302 monitors tilting through the four LVDTs, making tests more accurate. If the tilting exceeds 10% of the

303 specimen height, the machine stops automatically. The LDSM used is capable of testing the specimens

304 according to ASTM D3080-11 and BS 1377-7. Figure 4 shows the LDSM used.

305 The kaolin (Eckalite 1) used in this study is high-quality water washed china clay with controlled

306 particle size distribution and colour, manufactured under a quality system certified facility. For sample

307 preparation, the kaolin was mixed with water using a mechanical mixer and prepared at an average

308 water content, consistency index and liquidity index of 56%, 0.61 and 0.38, respectively. The

309 undrained shear strength (S_u), in kPa, of kaolin was estimated to be approximately 29.3 kPa using the

310 following correlation proposed by Wroth & Wood (1978):

311 $$S_u = 170 \text{ x exp } (-4.6 \text{ x LI})$$ (1)

312 where, LI is the liquidity index of the soil.

313 Afterwards, the prepared kaolin was thoroughly mixed and soaked for at least 24 hours in an airtight

314 container to ensure uniform water consistency. Necessary care was practised to prevent lumps from

315 being left in the prepared kaolin. The dry density of the kaolin bed was set constant to 10 kN/m^3 for

316 all the specimens. The kaolin bed was prepared by compacting the pre-weighted kaolin in three equal

317 layers spread and compacted evenly using a hand tamper to avoid any air entrapment between the

318 layers of kaolin. The thickness of each kaolin layer was maintained at 50 mm. Kaolin samples were

319 taken from the leftover of kaolin bed every time the specimen was prepared to determine the most

320 representative water content.

321   With a column penetration ratio (C_r), defined as the height of the column to the height of the

322   specimen, of 1.0, an end-bearing granular column was installed in the middle of the kaolin bed through

323   the replacement method. A thin-walled polyvinyl chloride (PVC) tube, with a thickness of 2.5 mm and

324   an external diameter of 68mm, was used to construct the granular column. The end-bearing column

325   was created because the increase in column length significantly improves the behaviour of reinforced

326   soil, mainly due to sufficient mobilisation of end-bearing capacity and skin resistance through an

327   increase in the peripheral area and overburden stress (Dash & Bora, 2013). An adequate gap was

328   maintained between the shear box and the boundaries of the granular column to avoid the boundary

329   effect during the test. The PVC tube was gradually pushed vertically and concentrically into the kaolin

330   bed until it reached the bottom of the shear box. A static force was applied to drive the PVC tube into

331   the kaolin to minimise the disturbance in the surrounding kaolin. After installing the PVC tube, the

332   kaolin within the tube was scooped out using a stainless steel spatula. All the geocomposites were

333   prepared at an area replacement ratio (A_r) of 16%. A_r is defined as the plan area of the column to the

334   plan area of the shear box. This A_r was selected to avoid the influence of the shear box boundary on

335   the results. The column's length to diameter (L/D) ratio was 2.2, ensuring that the column was within

336   its critical length. The pre-weighed quantity of oven-dried granular backfill was carefully charged into

337   the resulting hole using a funnel. The column backfill was compacted in three different layers using a

338   hand tamper to achieve a relative density (or density index) of 60%. This relative density was adopted

339   to ensure there was no lateral bulging of the column to avoid disturbance to the surrounding kaolin.

340   Another reason for choosing this relative density was to pick a value that correlates with the practical

341   conditions. The column backfill was compacted till both kaolin and column reached the same height.

342   Afterwards, the cylindrical PVC tube was gradually withdrawn from the kaolin bed by carefully pulling

343   it upwards. Samples were taken from the leftover of the prepared kaolin bed just before starting the

344   LDS test to perform the water content testing. The shearing plane was situated in the middle of the

345   sample (at 75 mm height). Overall, this procedure was found to give repeatable and uniform

346   specimens of good quality. The typical plan and cross-section of the geocomposite are shown in Figure

347   5a and 5b, respectively.

348   The single-stage (implying that a new specimen was prepared for test under each load) stress-

349   controlled LDS experiments were performed on the prepared kaolin specimens and geocomposites.

350   The geocomposites were tested separately under 12.5 kPa, 25 kPa, 50 kPa and 100 kPa normal stress,

351   with the normal stress increasing at a load increment factor of 1.0. All the geocomposites and kaolin

352   specimens were consolidated under each normal stress before shearing them uniformly at a slow rate

353   of 0.02 mm/min to allow the column to mobilise its drainage capacity. The specimens were allowed

354   to drain water and were not inundated during the test. The test was stopped when the shear stress

355   became constant, or the shear displacement reached 28 mm (18% shear strain). The stress and

356   displacement data were continuously recorded using the LVDT and computerised data acquisition

357   system. Altogether, sixteen LDS tests were performed. Figure 6a, 6b, 6c and 6d represents the top

358   view of the kaolin specimen, the NS-kaolin, the MS-kaolin and the CWG-kaolin geocomposite before

359   the test respectively.

360   **Experimental results**

361   The obtained results were used to develop the shear strength envelopes that were best-fitted using

362   the Coulomb failure criterion. The peak shear strength from each experiment was plotted against the

363   corresponding normal stress to develop the envelope. The shear strength of all the specimens was

364   found to increase with normal stress. The applied normal stresses and measured shear stresses were

365   corrected for reductions in the shearing area during the specimen shearing. The fitting parameters for

366   each envelope were determined in terms of the coefficient of determination (R^2) and the Nash-

367   Sutcliffe model efficiency coefficient (NSE). Given the criteria proposed by Chiew & McMahon (1993),

368   the goodness-of-fit of all shear strength envelopes presented in this paper can be rated as "perfect"

369   (NSE ≥ 0.93). Table 3 shows the peak friction angle of the kaolin specimens and the geocomposites.

370   Figure 7 shows the peak shear strength envelopes of the kaolin and the geocomposites.

371 The results show that the cohesion of kaolin is 1.7 kPa, whereas its friction angle is $14.0°$. Overall,

372 installing a granular column increased the shear strength of the geocomposite, regardless of the

373 type of column backfill used. The shear strength parameters of kaolin were considered as a

374 reference for comparison.

375 The results of the NS-kaolin geocomposite showed that installing the NS column increased the friction

376 angle from $14.0°$ to $17.8°$, an increase of 27%, whereas the cohesion increased over two-fold from 1.7

377 kPa to 3.9 kPa. Compared to the kaolin specimens, the increase in the friction angle of the NS-kaolin

378 geocomposite appears largely due to the inclusion of the NS column, as the characterisation testing

379 previously showed that NS has a peak friction angle of $36.9°$ under dry conditions. It is postulated that

380 the NS-kaolin geocomposite derives its cohesion (3.9 kPa) from two parts: the true cohesion of kaolin

381 and the apparent cohesion of NS.

382 The results of the MS-kaolin geocomposite showed an increase in both the cohesion and friction angle.

383 The friction angle of the MS-kaolin geocomposite increased to $17.7°$, an increase of 26%, which is

384 similar to that of the NS-kaolin geocomposite. However, the MS column considerably increased the

385 cohesion of the geocomposite to 5.4 kPa, an increase of over three-fold. Also, the peak shear strength

386 of the MS-kaolin geocomposite was higher than that of the NS-kaolin geocomposite under all the

387 applied normal stresses. The reason for the higher peak shear strength of the MS-kaolin geocomposite

388 compared with that of the NS-kaolin geoomposite could be the more well-graded MS, its higher

389 particle angularity and its larger median particle size.

390 The results of the CWG-kaolin geocomposite showed a two-fold increase in cohesion compared with

391 kaolin alone, which is somewhat similar to that of the NS-kaolin geocomposite. Importantly, installing

392 the CWG column showed the highest increase in friction angle, increasing from $14.0°$ for kaolin alone

393 to $20.7°$. The reason for the relatively higher friction angle of the CWG-kaolin geocomposite and lower

394 cohesion could be the higher Young's Modulus of the CWG particles. The Young's Modulus of CWG is

395 nearly 45 Gpa (Hsieh et al., 2009; University of Texas, 2019), whereas that of sands and gravels varies

396   from 10-170 MPa (University of Texas, 2019). The higher Young's Modulus of CWG potentially attracts

397   greater stress to the CWG column, leading to more stress being taken by the CWG column than the

398   kaolin. As a result, the granular characteristics of the geocomposite become more dominant during

399   shearing.

400   Figures 8a and 9a present the shear stress-horizontal displacement and horizontal-vertical

401   displacement behaviour of kaolin alone, respectively. Figures 8b, 8c and 8d present the shear stress-

402   horizontal displacement behaviour of NS-kaolin, MS-kaolin and CWG-kaolin geocomposites,

403   respectively. Similarly, Figures 9b, 9c and 9d present the horizontal-vertical displacement behaviour

404   of NS-kaolin, MS-kaolin and CWG-kaolin geocomposites, respectively. The shear stress-horizontal

405   displacement behaviour of the kaolin specimens showed that the shear stress non-linearly increased

406   with an increase in shear displacement. The horizontal-vertical displacement behaviour of the kaolin

407   specimens showed progressively higher vertical displacement with increasing normal stress, with over

408   10 mm compression observed under 100 kPa normal stress. It was also noted that the amount of

409   vertical displacement during shearing under higher normal stress (100 kPa) was highest in kaolin alone

410   compared to all of the geocomposites.

411   The shear stress-horizontal displacement behaviour of the NS-kaolin geocomposite showed a clear

412   peak in shear stress under 100 kPa normal stress. The horizontal-vertical displacement behaviour of

413   the NS-kaolin geocomposite showed that the lowest and highest vertical displacement occurred under

414   100 kPa and 50 kPa normal stress, respectively. A sharp drop in vertical stress was also noted in the

415   NS-kaolin geocomposite at approximately 17 mm horizontal displacement under 12.5 kPa normal

416   stress. This drop in vertical displacement would have densified the specimen, leading to a slight

417   increase in shear stress. The MS-kaolin geocomposite showed two distinct rises and falls in shear stress

418   between 1-3 mm horizontal displacement under 50 kPa normal stress, possibly due to the dispersion

419   of microcracks or rearrangement of sand particles. Another potential reason for these sudden changes

420   could be that some sand particles at the column-kaolin interface started to penetrate the kaolin,

421   leading to a sudden drop in shear stress. When the smear zone was created, the shear stress started

422   increasing again (Xu et al., 2018).

423   The horizontal-vertical displacement behaviour of the MS-kaolin geocomposite showed a drop in

424   vertical displacement between 12-13 mm and 20-21 mm horizontal displacement under 12.5 kPa

425   normal stress. This drop in vertical displacement would have densified the MS-kaolin geocomposite,

426   increasing the shear stress at these horizontal displacements, as for the NS-kaolin geocomposite. Also,

427   the shear stress-horizontal displacement behaviour of the CWG-kaolin geocomposite showed a

428   relatively higher increase in shear stress with increasing normal stress. A sharp rise and fall in shear

429   stress were also observed between 3-4 mm horizontal displacement under 50 kPa normal stress,

430   possibly due to localised strain-softening, which is somewhat comparable to the MS-kaolin

431   geocomposite results. Figure 9d shows a relatively smooth, non-linear and comparable horizontal-

432   vertical displacement behaviour under 12.5 kPa, 25 kPa and 100 kPa normal stress, with relatively

433   much higher vertical displacement under 50 kPa normal stress.

434   For all three geocomposites, the highest vertical displacement was observed under 50 kPa normal

435   stress, with the vertical displacement reducing under 100 kPa. The potential reason for this could be

436   greater stress concentration on the column under higher normal stresses, reducing the kaolin's

437   contribution to shear strength and allowing the column to dominate the system.

438   Figure 10 compares the maximum vertical displacement (compression) of all the specimens during

439   shearing with their corresponding applied normal stress. It can be seen that the significant reduction

440   in the maximum vertical displacement (less compression) occurs under the applied normal stress of

441   100kPa for all three geocomposites, potentially due to higher stress concentration on the column

442   under 100 kPa applied normal stress, which is the highest normal stress applied in this study.

443   **Discussion**

444   Typically, clays are highly sensitive to variation in their water content Spoor and Godwin (1979), and

445   are marked by lower shear strength (Aslani et al., 2019). This study observed that the kaolin has the

446   lowest direct shear strength. It was also noted that the inclusion of granular column increased the

447   shear strength of the geocomposite, regardless of the type of column backfill, due to the combined

448   soil-granular column system, which has been observed by several researchers before (Mohapatra et

449   al., 2016). For example, reinforcing the kaolin with the CWG column under the applied normal stresses

450   of 12.5, 25, 50 and 100 kPa increased the shear strength from 5.7, 9.9, 15.7 and 33.2 kPa to 8.9, 13.1,

451   29.9 and 49.3 kPa, respectively. As granular columns are formed by materials possessing relatively

452   higher friction angle, the treated soil-column matrix manifest a higher friction angle than untreated

453   soil, which is observed in the results presented in this study. Besides reinforcement, the increase in

454   shear strength due to granular column inclusion could partly be due to the drainage ability of columns,

455   causing a reduction in pore water pressure and an increase in effective stress of the soil (Najjar et al.,

456   2010).

457   The obtained shear strength results reflect the overall response of the entire test specimens. The

458   results showed that the increase in shear strength caused by the NS or MS column is comparable to

459   each other, showing close peak friction angle values of 17.8º and 17.7º for the NS-kaolin and the MS-

460   kaolin geocomposite, respectively. The peak shear strength of the MS-kaolin geocomposite was higher

461   than that of the NS-kaolin geocomposite. The potential reason for this finding could be the more well-

462   graded gradation of MS, favouring the development of higher peak shear stress (Siahaan et al., 2018).

463   Another potential reason could be the relatively higher angularity of the MS particles Kazmi et al.

464   (2021), leading to a superior interlock between the MS particles. Naeini and Gholampoor (2019)

465   investigated the shear strength behaviour of stone column-treated wet clays by installing ordinary

466   stone columns and geotextile-encased stone columns using three different sizes of stones, ranging 1-

467   2 mm, 2-5 mm and 5-8 mm. Their study found that the wet clay reinforced with columns containing

468   coarser stones showed relatively greater shear strength than those containing smaller aggregates,

469   potentially due to the higher friction angle of coarser stones. Similarly, Bareither et al. (2008) analysed

470   the physical properties and shear strength of 30 compacted sands sourced from a wide range of

471   geological deposits. Their study concluded that sands with the highest friction angle tend to have

472   coarser particles, well-graded gradation and/or angular particle shape. Hence, previous studies

473   support the results of this paper, as MS-kaolin geocomposite showed a higher shear strength than

474   that of the NS-kaolin geocomposite.

475   Installing the CWG column caused a relatively higher increase in the peak shear strength of the

476   geocomposite under higher normal stresses; this is reflected in the results of the CWG-kaolin

477   geocomposite, showing the highest friction angle and the lowest cohesion among the three

478   geocomposites. For example, the shear strength mobilised by the CWG-kaolin geocomposite under 50

479   and 100 kPa normal stress were higher than that of the other two geocomposites. Secondly, installing

480   the CWG column increased the friction angle from 14.0° to 20.7° (48% increase) compared to that of

481   kaolin only. This notable increase in the friction angle caused by installing the CWG column suggests

482   that the frictional resistance provided by the CWG column was an important factor contributing to the

483   overall increase in the shear strength of the CWG-kaolin geocomposite. Technically, there is a

484   significant difference in the Young's modulus of glass compared to that of traditional sands. Literature

485   shows that the Young's Modulus of CWG is nearly 45 GPa (Hsieh et al., 2009; University of Texas,

486   2019), whereas that of sands and gravels varies from 10-170 Mpa (University of Texas, 2019). The

487   potential reason for the highest increase in shear strength of the CWG-kaolin geocomposite could be

488   the higher stiffness (Young's modulus) of CWG particles, causing relatively higher stress concentration

489   on the CWG column, ultimately leading to more stress being taken by the CWG column than

490   surrounding kaolin.

491   The post-shearing cross-section of the geocomposites under 25 kPa applied normal stress are given in

492   Figure 11. These cross-sectional photos were taken by splitting the geocomposites along their vertical

493   axes to reveal the column and the surrounding kaolin. Upon careful examination of the geocomposites

494   after shearing, it was noted that all three geocomposites underwent shear failure by lateral separation

495   at the shearing plane. This finding complies with the previous literature, suggesting that a short

496   column resting on a firm stratum typically fails in shear (Barksdale & Bachus, 1983). Further, it was

497   observed that the CWG-kaolin geocomposite showed some signs of column bulging, largely at the

498   centre. This finding supports the hypothesis that the CWG column attracted relatively higher stress

499   concentration due to the mentioned higher stiffness of CWG particles, causing the CWG column to

500   mobilise greater passive resistance from surrounding kaolin than the NS or MS column.

501   The use of encasement with granular columns is a fairly common technique to improve their

502   performance, particularly in soft soils. Typically, geosynthetic materials (geotextiles and geogrids) are

503   suited for use as encasements due to their superior tensile characteristics. Geosynthetic encasement

504   could also improve the lateral load capacity of the granular column by developing hoop tension forces

505   in the encasement layer, giving additional confinement to the column material (Mohapatra et al.,

506   2016). As a result, they minimise the chances for bulging failure and for penetration of column material

507   into the surrounding soil that could inhibit the drainage ability of the column (Dutta et al., 2016). As

508   this study is among the first to investigate the performance of a granular column based on its type of

509   column backfilling material (NS, MS or CWG), it was logical not to encase the granular column during

510   the tests, providing benchmark results excluding the effect of the encasement. Previous studies also

511   show that ordinary granular columns are prone to shear rupture under lateral soil movement and

512   ideally need some encasement to reduce the chances of rupturing under shear loading (Murugesan &

513   Rajagopal, 2009). Hence, future studies could consider investigating the direct shear behaviour of

514   similar geocomposites with an encased column, particularly for granular columns made up of CWG.

515   The next stage of this research will present results showing the effect of particle size of CWG on the

516   geotechnical behaviour of kaolin reinforced with a CWG column.

517   **Conclusion**

518   This study investigated the shear strength behaviour of column-kaolin geocomposites containing a

519   column made up of NS, MS or CWG installed in the middle of the kaolin bed. Overall, installing a

520   granular column increased the shear strength of the geocomposite, regardless of the type of column

521   backfill used. It was observed that the increase in shear strength along the horizontal plane at the mid-

522   height of the geocomposite inside the shear box caused by installing the NS or MS column was

523   relatively comparable to each other, with the MS-kaolin geocomposite showing shear strength higher

524   than that of the NS-kaolin geocomposite under all the applied normal stresses. A potential reason for

525   this finding could be the well-graded gradation, higher particle angularity and larger median particle

526   size of the MS than the NS. The results also showed that the CWG column is relatively more effective

527   at increasing the peak shear strength of the geocomposite under higher normal stresses. It was noted

528   that installing the CWG column led to the highest increase in the friction angle of the geocomposite.

529   This could potentially be due to the higher stiffness of the CWG particles than that of the NS and the

530   MS particles, causing greater stress concentration on the CWG column, ultimately leading to more

531   stress being taken by the CWG column than the surrounding kaolin. Given the favourable performance

532   demonstrated by the CWG column in this study, it is recommended to compare the experimental

533   results of this study with field performance and large-scale physical model tests containing NS, MS or

534   CWG columns. Secondly, this study suggests investigating the geotechnical behaviour of kaolin

535   reinforced with groups of CWG columns. Given that this study is among the first to study the shear

536   strength behaviour of CWG columns in clayey soil, it is also suggested for future researchers to study

537   how CWG columns behave when encased with a suitable geosynthetic material. This study supports

538   performing a detailed quantitative economic and environmental feasibility investigation for using

539   CWG as column backfill in granular columns for future studies.

540   **Data Availability Statement**

541   All data, model, and code that support the findings of this study are available from the corresponding

542   author upon reasonable request.

552 **Notation**

553 The following symbols are used in this paper:

554 LDS   Large direct shear test

555 NS   Natural sand

556 MS   Manufactured sand

557 CWG   Crushed waste glass

558 LDSM   Large direct shear test machine

559 LVDT   Linear variable differential transducers

560 S_U Undrained shear strength

561 C_r Column penetration ratio

562 PVC   Polyvinyl Chloride

563 A_r Area replacement ratio

564 L/D ratio   Length to Diameter ratio

565 NSE   Nash-Sutcliffe model efficiency coefficient

566 **References**

567 Abhishek, Rajyalakshmi, & Madhav. (2016). Engineering of ground with granular piles: a critical

568   review. *International Journal of Geotechnical Engineering, 10*(4), 337-357.

569 Afshar, & Ghazavi. (2014). A simple analytical method for calculation of bearing capacity of stone-

570   column. *International Journal of Civil Engineering, 12*(1), 15-25.

571 Afshar, Hemmati, & Azimi. (2010). Laboratory Investigation on the Effect of Sand Columns on the

572   Shear Strength of Soft Soil *Geo-Chicago 2016* (pp. 807-815).

573 Alfaro, Balasubramaniam, Bergado, & Chai. (1994). *Improvement techniques of soft ground in*

574   *subsiding and lowland environment*: CRC Press.

575   Ali. (2012). *Geotechnical characteristics of recycled glass in road pavement applications.* Doktora

576   Tezi, Swinburne University of Technology, Melbourne, Australia.

577   Alnunu, & Nalbantoglu. (2019). Performance of loose sand with different waste materials in stone

578   columns in North Cyprus. *Environmental Geotechnics*, 1-6.

579   Amini. (2016). *Physical modelling of vibro stone column using recycled aggregates.* University of

580   Birmingham.

581   Andreou, Frikha, Frank, Canou, Papadopoulos, & Dupla. (2008). Experimental study on sand and

582   gravel columns in clay. *Proceedings of the Institution of Civil Engineers-Ground Improvement,*

583   *161*(4), 189-198.

584   Aslani, Nazariafshar, & Ganjian. (2019). Experimental study on shear strength of cohesive soils

585   reinforced with stone columns. *Geotechnical and Geological Engineering, 37*(3), 2165-2188.

586   Ayothiraman, & Soumya. (2015). Model tests on the use of tyre chips as aggregate in stone columns.

587   *Proceedings of the Institution of Civil Engineers-Ground Improvement, 168*(3), 187-193.

588   Babu, Nayak, & Shivashankar. (2013). A critical review of construction, analysis and behaviour of

589   stone columns. *Geotechnical and Geological Engineering, 31*(1), 1-22.

590   Bareither, Edil, Benson, & Mickelson. (2008). Geological and physical factors affecting the friction

591   angle of compacted sands. *Journal of Geotechnical and Geoenvironmental Engineering,*

592   *134*(10), 1476-1489.

593   Barksdale, & Bachus. (1983). *Design and construction of stone columns, vol. I*. Retrieved from

594   Barmade, Kale, & Gadekar. (2021). *Experimental Study on Load-Settlement Behaviour of Granular*

595   *Stone Column in Expansive Soil.* Paper presented at the Proceedings of the Indian

596   Geotechnical Conference 2019.

597   Bendixen, Best, Hackney, & Iversen. (2019). Time is running out for sand: Nature Publishing Group.

598   Bergado, Singh, Sim, Panichayatum, Sampaco, & Balasubramaniam. (1990). Improvement of soft

599   Bangkok clay using vertical geotextile band drains compared with granular piles. *Geotextiles*

600   *and Geomembranes, 9*(3), 203-231.

601   Bravo, De Brito, Pontes, & Evangelista. (2015). Mechanical performance of concrete made with

602   aggregates from construction and demolition waste recycling plants. *Journal of Cleaner*

603   *Production, 99*, 59-74.

604   Canakci, Celik, & Edil. (2017). Effect of sand column on compressibility and shear strength properties

605   of peat. *European Journal of Environmental and Civil Engineering*, 1-12.

606   Castro. (2017). Modeling stone columns. *Materials, 10*(7), 782.

607   Chawla, Raju, & Krishna. (2010). *Some environmental benefits of dry vibro stone columns in a gas*

608   *based power plant project.* Paper presented at the Indian Geotechnical Conference.

609   Mumbai, India: gndec. ac. in.

610   Chiew, & McMahon. (1993). Assessing the adequacy of catchment streamflow yield estimates. *Soil*

611   *Research, 31*(5), 665-680.

612   Clean Washington Center. (1996). *Best Practices in Glass Recycling - Analysis of Glass Dusts*.

613   Retrieved from

614   http://citeseerx.ist.psu.edu/viewdoc/download;jsessionid=8EA266C3CB54A9A2141B63AAB2

615   EDBA2C?doi=10.1.1.384.5175&rep=rep1&type=pdf

616   Dash, & Bora. (2013). Influence of geosynthetic encasement on the performance of stone columns

617   floating in soft clay. *Canadian Geotechnical Journal, 50*(7), 754-765.

618   Dutta, Nadaf, Lal Birali, & Mandal. (2016). Encased stone columns for soft ground improvement *Geo-*

619   *Chicago 2016* (pp. 746-755).

620   Egan, & Slocombe. (2010). Demonstrating environmental benefits of ground improvement.

621   *Proceedings of the Institution of Civil Engineers-Ground Improvement, 163*(1), 63-69.

622   Gourley, Newill, & Schreiner. (1993). *Expansive soils: TRL's research strategy.* Paper presented at the

623   Proc., 1st Int. Symp. on Engineering Characteristics of Arid Soils.

624   Hanna, Etezad, & Ayadat. (2013). Mode of failure of a group of stone columns in soft soil.

625   *International Journal of Geomechanics, 13*(1), 87-96.

626   Holmstrom, & Swan. (1999). *Geotechnical properties of innovative, synthetic lightweight aggregates.*

627   Paper presented at the Proceedings of the 1999 International Ash Utilization Symposium,

628   Lexington, KY.

629   Hsieh, Lin, Su, & Jang. (2009). Glass forming ability and mechanical properties characterization on

630   Mg58Cu31Y11– xGdx bulk metallic glasses. *Journal of alloys and compounds, 483*(1-2), 40-

631   43.

632   Kazmi, Serati, Williams, Qasim, & Cheng. (2020a). The potential use of crushed waste glass as a

633   sustainable alternative to natural and manufactured sand in geotechnical applications.

634   *Journal of Cleaner Production*, 124762.

635   Kazmi, Serati, Williams, Qasim, & Cheng. (2021). The potential use of crushed waste glass as a

636   sustainable alternative to natural and manufactured sand in geotechnical applications.

637   *Journal of Cleaner Production, 284*, 124762.

638   Kazmi, Serati, Williams, Qasim, Cheng, & Olaya. (2020b). *A Comparative Study on Shear Strength of*

639   *Crushed Waste Glass with Natural and Manufactured Sand.* Paper presented at the 54th US

640   Rock Mechanics/Geomechanics Symposium.

641   Kazmi, Serati, Williams, Qasim, Cheng, & Olaya. (2020c). *A Comparative Study on Shear Strength of*

642   *Crushed Waste Glass with Natural and Manufactured Sand.* Paper presented at the 54th US

643   Rock Mechanics/Geomechanics Symposium.

644   Kazmi, Williams, & Serati. (2019a). *Comparison of Basic Geotechnical Parameters of Crushed Waste*

645   *Glass with Natural and Manufactured Sands.* Paper presented at the 53rd US Rock

646   Mechanics/Geomechanics Symposium.

647   Kazmi, Williams, & Serati. (2019b). Waste Glass in Civil Engineering Applications–A Review.

648   *International Journal of Applied Ceramic Technology*.

649   Kumar, & Sadana. (2012). Bearing capacity of soil reinforced with vertical columns of recycled

650   concrete aggregates. *Australian Journal of Civil Engineering, 10*(2), 153-162.

651   Langer, Drew, & Sachs. (2004). Aggregate and the environment: American Geological Institute

652   Environmental Awareness, Series No. 8. *American Geological Institute, Alexandria, VA*.

653   Malarvizhi. (2007). Comparative study on the behavior of encased stone column and conventional

654   stone column. *Soils and Foundations, 47*(5), 873-885.

655   Manohar, & Patel. (2021). Ground Improvement with Stone Columns–A Review *Advances in Civil*

656   *Engineering* (pp. 197-217): Springer.

657   McCabe, McNeill, & Black. (2007). Ground improvement using the vibro-stone column technique.

658   Mehrannia, Kalantary, & Ganjian. (2018). Experimental study on soil improvement with stone

659   columns and granular blankets. *Journal of Central South University, 25*(4), 866-878.

660   Mishra, Bore, Jiang, Scheuermann, & Li. (2018a). Dielectric spectroscopy measurements on kaolin

661   suspensions for sediment concentration monitoring. *Measurement, 121*, 160-169.

662   Mishra, Scheuermann, & Li. (2018b). Significance of corrections and impact of saline pore fluid on

663   kaolin. *Journal of Materials in Civil Engineering, 30*(11), 06018016.

664   Mishra, Zhang, Bhuyan, & Scheuermann. (2020). Anisotropy in volume change behaviour of soils

665   during shrinkage. *Acta Geotechnica, 15*(12), 3399-3414.

666   Mitchell. (1970). In-place treatment of foundation soils. *Journal of Soil Mechanics & Foundations Div,*

667   *97*(SM1).

668   Mohapatra, Rajagopal, & Sharma. (2014). *Analysis of geotextile-reinforced stone columns subjected*

669   *to lateral loading.* Paper presented at the Proc. 10th Int. Conf. on Geosynthetics, Berlin,

670   Germany.

671   Mohapatra, Rajagopal, & Sharma. (2016). Direct shear tests on geosynthetic-encased granular

672   columns. *Geotextiles and Geomembranes, 44*(3), 396-405.

673   Mokhtari, & Kalantari. (2012). Soft Soil Stabilization using Stone Column--A Review. *Electronic*

674   *journal of Geotechnical engineering, 17*, 1459-1466.

675   Murugesan, & Rajagopal. (2007). Model tests on geosynthetic-encased stone columns.

676   *Geosynthetics International, 14*(6), 346-354.

677 Murugesan, & Rajagopal. (2009). Shear load tests on stone columns with and without geosynthetic

678   encasement. *Geotechnical Testing Journal, 32*(1), 76-85.

679 Naeini, & Gholampoor. (2019). Effect of Geotextile Encasement on the Shear Strength Behavior of

680   Stone Column-Treated Wet Clays. *Indian Geotechnical Journal, 49*(3), 292-303.

681 Najjar. (2013). A state-of-the-art review of stone/sand-column reinforced clay systems. *Geotechnical*

682   *and Geological Engineering, 31*(2), 355-386.

683 Najjar, Sadek, & Maakaroun. (2010). Effect of sand columns on the undrained load response of soft

684   clays. *Journal of Geotechnical and Geoenvironmental Engineering, 136*(9), 1263-1277.

685 Ng, & Tan. (2015). Stress transfer mechanism in 2D and 3D unit cell models for stone column

686   improved ground. *International Journal of Geosynthetics and Ground Engineering, 1*(1), 3.

687 Poorooshasb, & Meyerhof. (1997). Analysis of behavior of stone columns and lime columns.

688   *Computers and Geotechnics, 20*(1), 47-70.

689 Priebe. (1995). The design of vibro replacement. *Ground engineering, 28*(10), 31.

690 Ranjan. (1989). Ground treated with granular piles and its response under load. *Indian Geotechnical*

691   *Journal, 19*(1), 1-86.

692 Rossato, Ninis, & Jardine. (1992). Properties of some kaolin-based model clay soils. *Geotechnical*

693   *Testing Journal, 15*(2), 166-179.

694 Saberian, Li, & Cameron. (2019). Effect of crushed glass on behavior of crushed recycled pavement

695   materials together with crumb rubber for making a clean green base and subbase. *Journal of*

696   *Materials in Civil Engineering, 31*(7), 04019108.

697 Serridge. (2004). THE USE OF RECYCLED AGGREGATES IN VIBRO STONE COLUMN GROUND

698   IMPROVEMENT TECHNIQUES *Sustainable Waste Management and Recycling: Construction*

699   *Demolition Waste* (pp. 213-224): Thomas Telford Publishing.

700 Serridge, & Sarsby. (2009). Assessment of the use of recycled aggregates in vibro-stone column

701   ground improvement techniques *Construction for a Sustainable Environment* (pp. 86-101):

702   CRC Press.

703 Serridge, & Slocombe. (2012). Chapter 84 Ground improvement *ICE manual of geotechnical*

704   *engineering* (pp. 1247-1269): Thomas Telford Ltd.

705 Shahverdi, & Haddad. (2020). Use of recycled materials in floating stone columns. *Proceedings of the*

706   *Institution of Civil Engineers-Construction Materials, 173*(2), 99-108.

707 Siahaan, Indraratna, Ngo, Rujikiatkamjorn, & Heitor. (2018). Influence of Particle Gradation and

708   Shape on the Performance of Stone Columns in Soft Clay. *Geotechnical Testing Journal,*

709   *41*(6), 1076-1091.

710 Sivakumar, O'Kelly, Moorhead, Madhav, & Mackinnon. (2014). Effectiveness of granular columns in

711   containing settlement. *Proceedings of the Institution of Civil Engineers-Geotechnical*

712   *Engineering, 167*(4), 371-379.

713 Spoor, & Godwin. (1979). Soil deformation and shear strength characteristics of some clay soils at

714   different moisture contents. *Journal of Soil Science, 30*(3), 483-498.

715 University of Texas. (2019). Some Useful Numbers on the Engineering Properties of Materials

716   (Geologic and Otherwise) GEOL 615.   Retrieved from

717   https://www.jsg.utexas.edu/tyzhu/files/Some-Useful-Numbers.pdf

718 Wang. (2009). Consolidation of soft clay foundations reinforced by stone columns under time-

719   dependent loadings. *Journal of Geotechnical and Geoenvironmental Engineering, 135*(12),

720   1922-1931.

721 Wroth, & Wood. (1978). The correlation of index properties with some basic engineering properties

722   of soils. *Canadian Geotechnical Journal, 15*(2), 137-145.

723 Xu, Methiwala, Williams, & Serati. (2018). Strength and consolidation characteristics of clay with

724   geotextile-encased sand column. *Proceedings of the Institution of Civil Engineers-Ground*

725   *Improvement, 171*(3), 125-134.

726 Zukri, & Nazir. (2018). Sustainable materials used as stone column filler: A short review. *MS&E,*

727   *342*(1), 012001.

728

729 # Tables

730 **Table 1**. Results of mineralogical analysis performed using XRF spectroscopy (Kazmi et al., 2021).

Oxide concentration	Units	Natural sand	Manufactured sand	Crushed waste glass
SiO_2	%	99.81	67.74	72.07
TiO_2	%	0.06	0.67	0.05
Al_2O_3	%	<0.01	16.17	1.45
Fe_2O_3	%	0.05	5.81	0.34
MnO	%	<0.01	0.12	0.01
MgO	%	0.03	2.13	0.69
CaO	%	0.01	1.38	11.09
Na_2O	%	<0.01	1.71	13.73
K_2O	%	0.01	3.72	0.33
P_2O_5	%	91.07	0.16	0.03
SO_3	%	82.43	0.24	0.09
V_2O_5	ppm	9	177	20
Cr_2O_3	ppm	11	97	539
ZnO	ppm	5	122	72
SrO	ppm	2	133	155
BaO	ppm	26	920	355
Co_3O_4	ppm	42	18	26
NiO	ppm	8	42	4
CuO	ppm	<2	37	4

731

732 **Table 2.** Geotechnical parameters of the materials (Adapted from Kazmi et al. (2021) and Xu et al.
733 (2018))

Parameter	NS	MS	CWG	Kaolin	Standards
C_u	1.43	13.37	2.21	-	-
C_c	0.94	1.51	0.96	-	-
Minimum dry density (dry placement method) (kg/m^3)	1540	1690	1390	-	AS 1289.5.5.1–1998
Maximum dry density (Wet placement method) (kg/m^3)	1650	1960	1820	-	AS 1289.5.5.1–1998
Hydraulic conductivity (m/s)	3.81×10^{-4}	3.59×10^{-4}	4.01×10^{-4}	-	ASTM D2434-68
Abrasion loss (%)	6.00	9.60	2.40	-	ASTM D7428
Critical-state friction angle under dry conditions (º)	31.1	44.1	29.1	-	AS 1289.6.2.2-1998
Critical-state friction angle under saturated conditions (º)	30.7	41.3	32.4	-	AS 1289.6.2.2-1998
Particle roundness index	0.55 (Rounded)	0.24 (Sub-angular)	0.32 (Sub-rounded)	-	-
Specific gravity	2.63	2.74	2.50	2.61	ASTM D5550
Median particle size (mm)	0.29	1.55	1.42	0.0012	AS 1289.3.6.1-2009
Liquid limit (%)	-	-	-	90	ASTM D4318 - 10
Plastic limit (%)	-	-	-	35	ASTM D4318 - 10
Plasticity index (%)	-	-	-	55	ASTM D4318 - 10
F_{200} (%)	-	-	-	69	
Unified soil classification system (USCS) rating	SP	SW	SP	CH	ASTM D2487 - 06

734

735 **Table 3.** Comparison of the shear strength of kaolin with geocomposites

	Kaolin	NS-kaolin geocomposite	MS-kaolin geocomposite	CWG-kaolin geocomposite
Cohesion (kPa)	1.7	3.9	5.4	3.1
Angle of internal friction (º)	14.0	17.8	17.7	20.7

Figure captions

736

737   **Fig.1.** Installation of the granular column through dry bottom-feed technique (Adapted from (Serridge

738   & Slocombe, 2012))

739   **Fig.2.** Optical microscopic images of NS, MS and CWG (from left to right)

740   **Fig.3.** Gradation curve of the test materials (Adapted from Kazmi et al. (2021) and Xu et al. (2018))

741   **Fig.4.** Large direct shear machine (Wille Geotechnik ADS-300)

742   **Fig.5a.** Typical plan of the geocomposite

743   **Fig.5b.** Typical cross-section of the geocomposite

744   **Fig.6a.** Experimental set up prepared in the shear box for kaolin specimen

745   **Fig.6b.** Experimental set up prepared in the shear box for NS-kaolin geocomposite

746   **Fig.6c.** Experimental set up prepared in the shear box for MS-kaolin geocomposite

747   **Fig.6d.** Experimental set up prepared in the shear box for CWG-kaolin geocomposite

748   **Fig.7.** Peak shear strength envelopes of kaolin and the geocomposites

749   **Fig.8a.** Shear stress-horizontal displacement behaviour of kaolin

750   **Fig.8b.** Shear stress-horizontal displacement behaviour of NS-kaolin geocomposite

751   **Fig.8c.** Shear stress-horizontal displacement behaviour of MS-kaolin geocomposite

752   **Fig.8d.** Shear stress-horizontal displacement behaviour of CWG-kaolin geocomposite

753   **Fig.9a.** Horizontal-vertical displacement behaviour of kaolin specimen

754   **Fig.9b.** Horizontal-vertical displacement behaviour of NS-kaolin geocomposite

755   **Fig.9c.** Horizontal-vertical displacement behaviour of MS-kaolin geocomposite

756   **Fig.9d.** Horizontal-vertical displacement behaviour of CWG-kaolin geocomposite

757   **Fig.10.** Maximum vertical displacement-normal stress behaviour of the specimens

758   **Fig.11.** Post-shearing cross-section of the geocomposites under 25 kPa normal stress (NS-kaolin, MS-

759   kaolin and CWG-kaolin geocomposite from left to right)

760

761

Step 1
Penetration

Step 2
Delivery

Step 3
Compaction

Step 4
Finishing

762

763   **Fig.1.** Installation of the granular column through dry bottom-feed technique (Adapted from

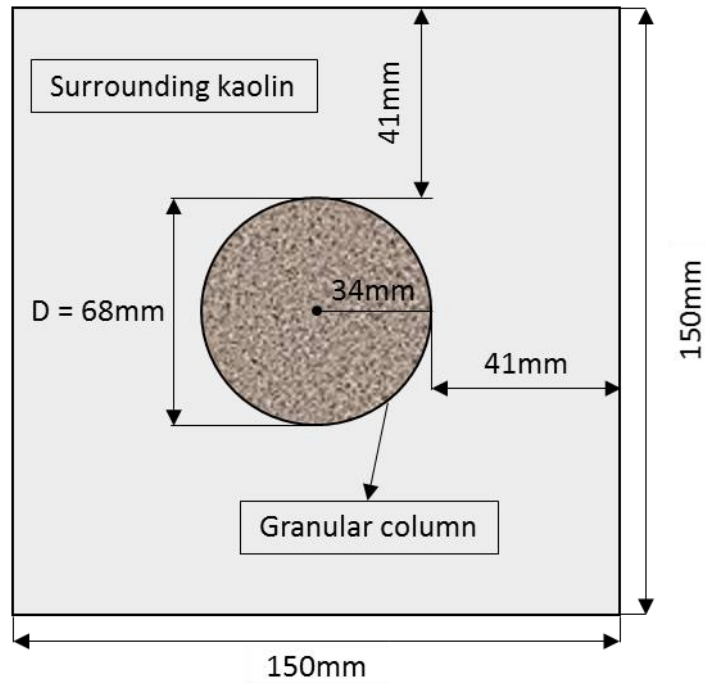764   (Serridge & Slocombe, 2012))

765

766

767

768
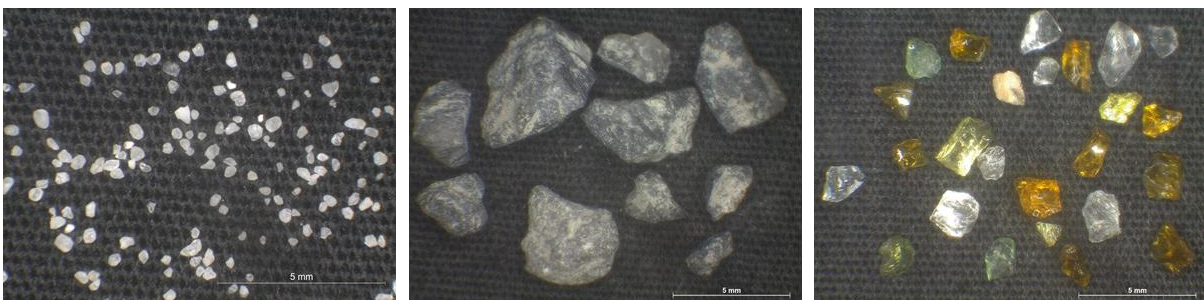
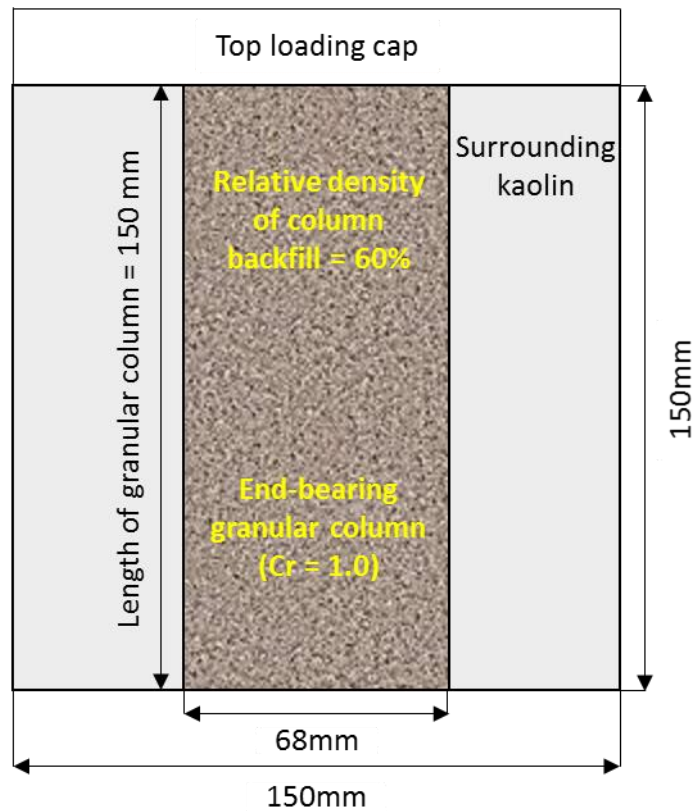769   **Fig.2.** Optical microscopic images of NS, MS and CWG (from left to right)

770

771

Fig.2. Gradation curve of the test materials (Adapted from Kazmi et al. (2021) and Xu et al. (2018))

773

774

Fig.4. Large direct shear machine (Wille Geotechnik ADS-300)

776

Fig.5a. Typical plan of the geocomposite

Fig.5b. Typical cross-section of the geocomposite

811
812
813
814
815
816
817
818
819
820
821
822

Fig.6a. Pure kaolin sample prepared in the shear box

823
824
825
826
827
828
829
830
831
832
833
834

Fig.6b. NS-kaolin geocomposite prepared in the shear box

835
836
837
838
839
840
841
842
843
844
845
846
847
848
849
850
851

Fig.6c. MS-kaolin geocomposite prepared in the shear box

852
853
854
855
856
857
858
859
860
861
862
863
864
865
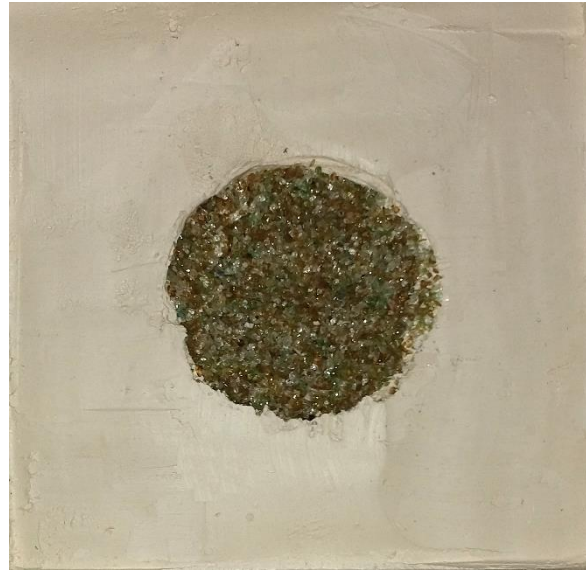
Fig.6d. CWG-kaolin geocomposite prepared in the shear box

866
867
868
869
870
871
872
873
874
875
876
877
878
879
880
881
882
883
884
885
886
887
888
889
890
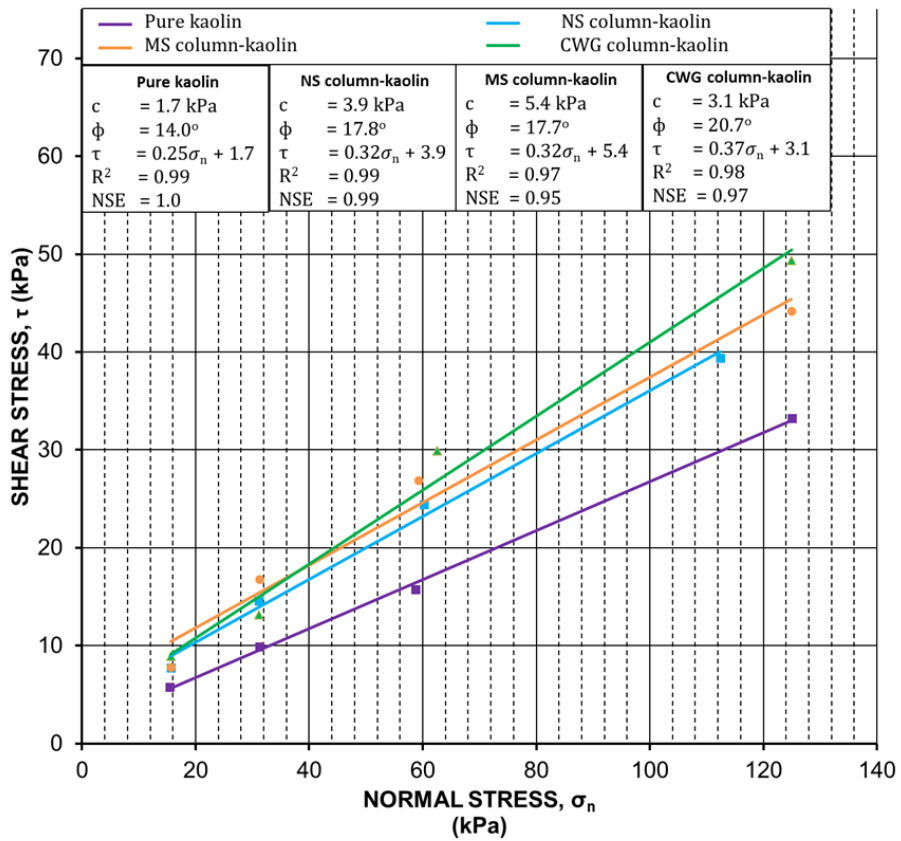
Fig.7. Peak shear strength envelopes of pure kaolin and the geocomposites
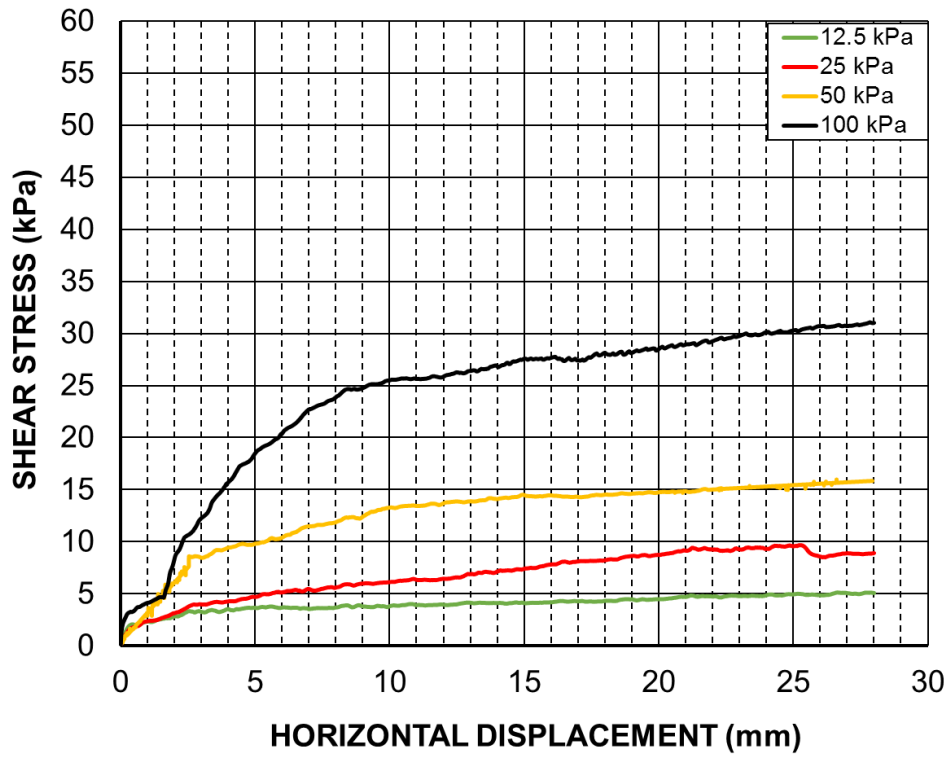
Fig.8a. Shear stress-horizontal displacement behaviour of pure kaolin sample
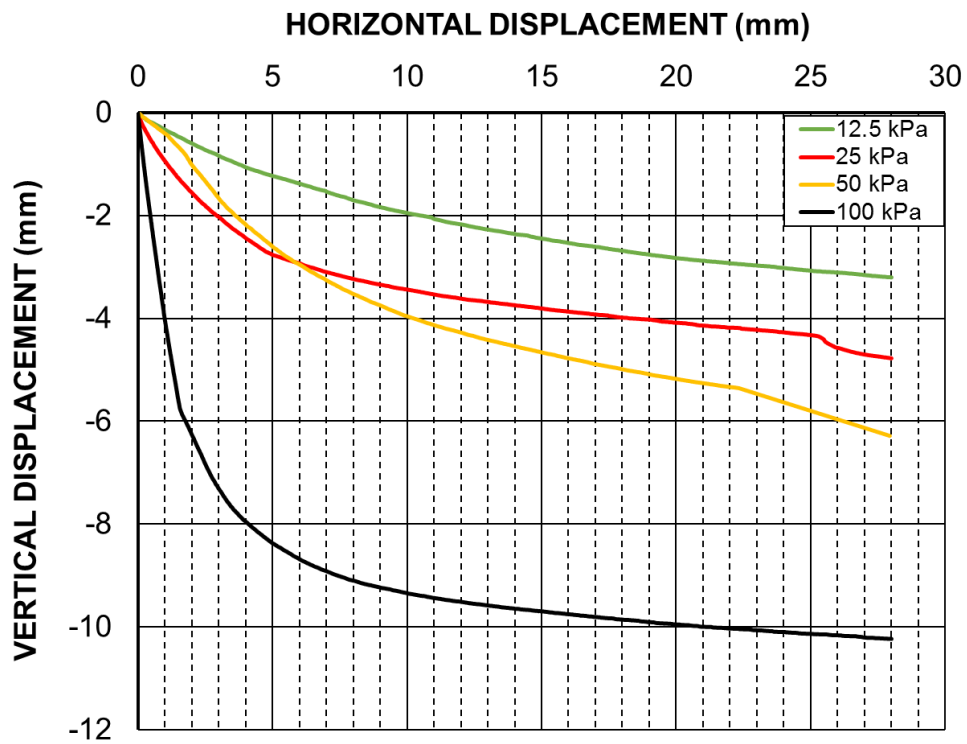
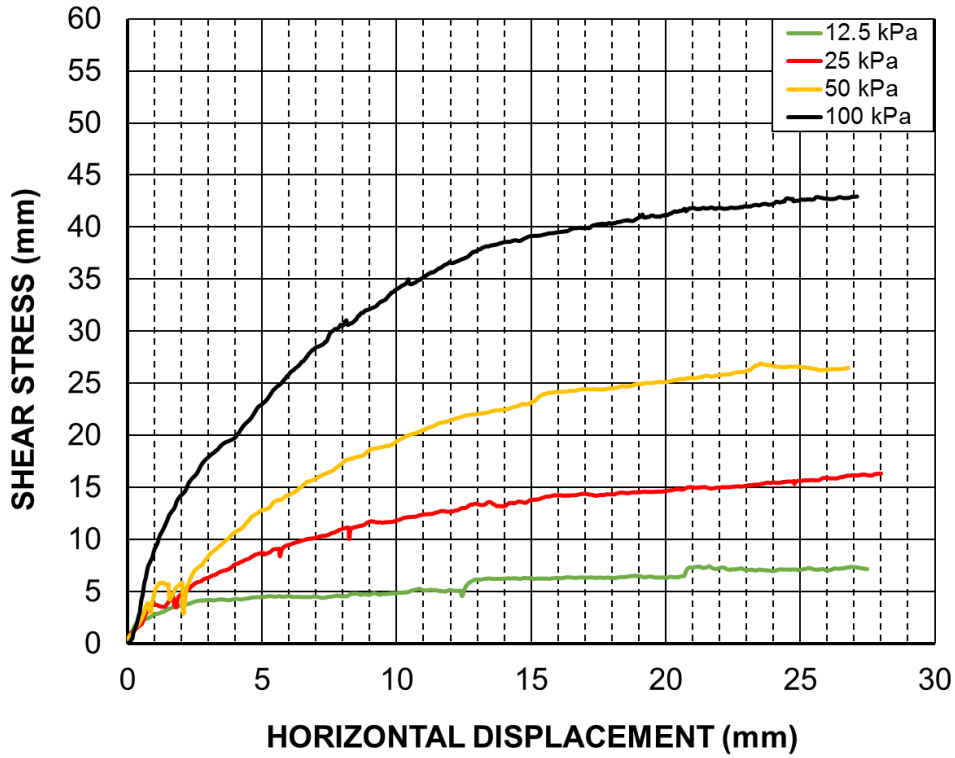**Fig.9a.** Horizontal-vertical stress displacement behaviour of pure kaolin sample
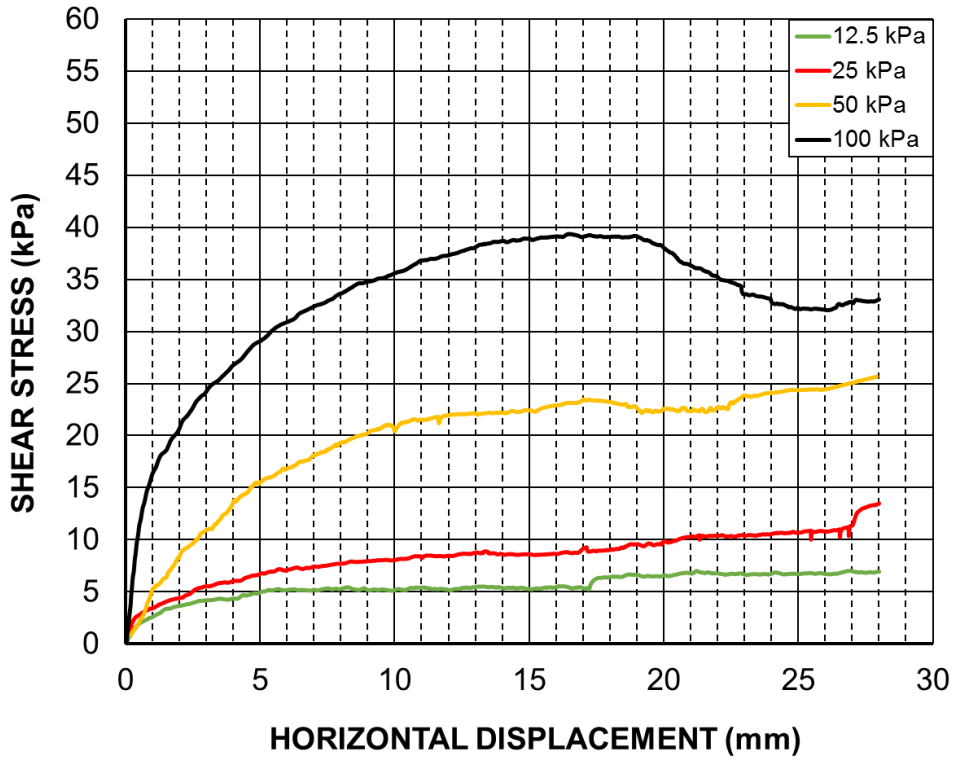
895
896   **Fig.8b.** Shear stress-horizontal displacement behaviour of NS-kaolin geocomposite
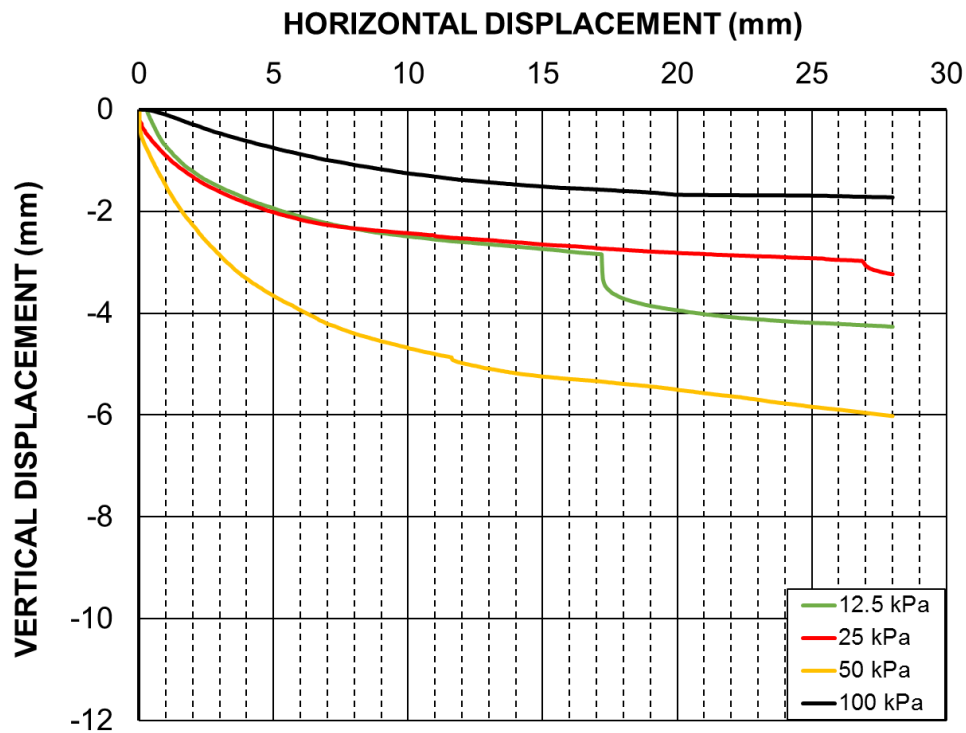
897   **Fig.9b.** Horizontal-vertical stress displacement behaviour of NS-kaolin geocomposite
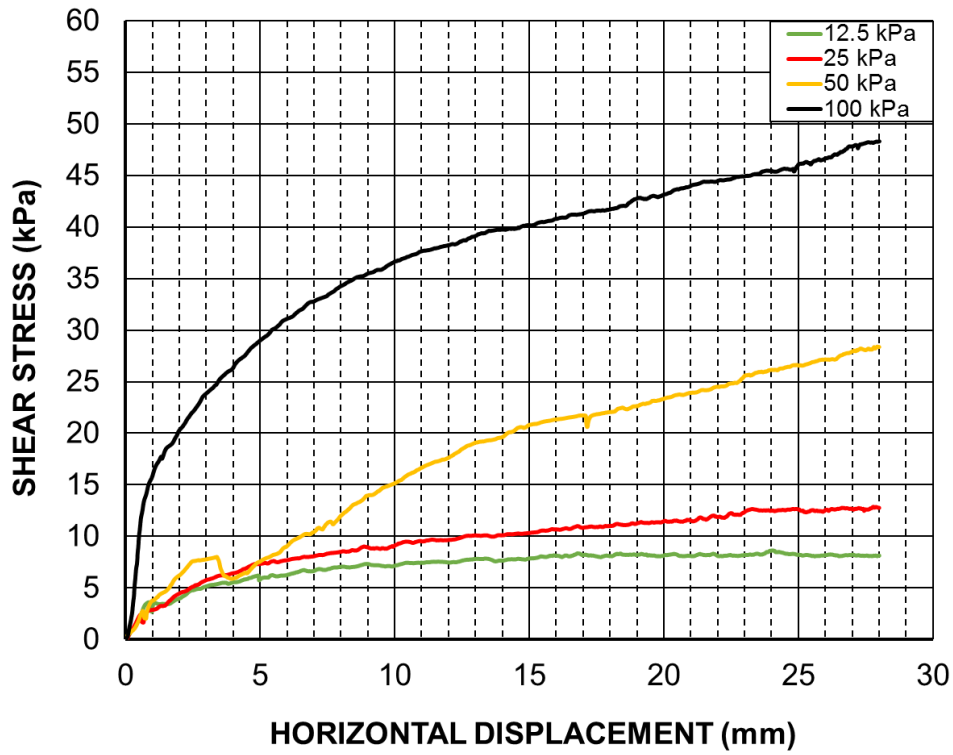898

899   **Fig.8c.** Shear stress-horizontal displacement behaviour of MS-kaolin geocomposite
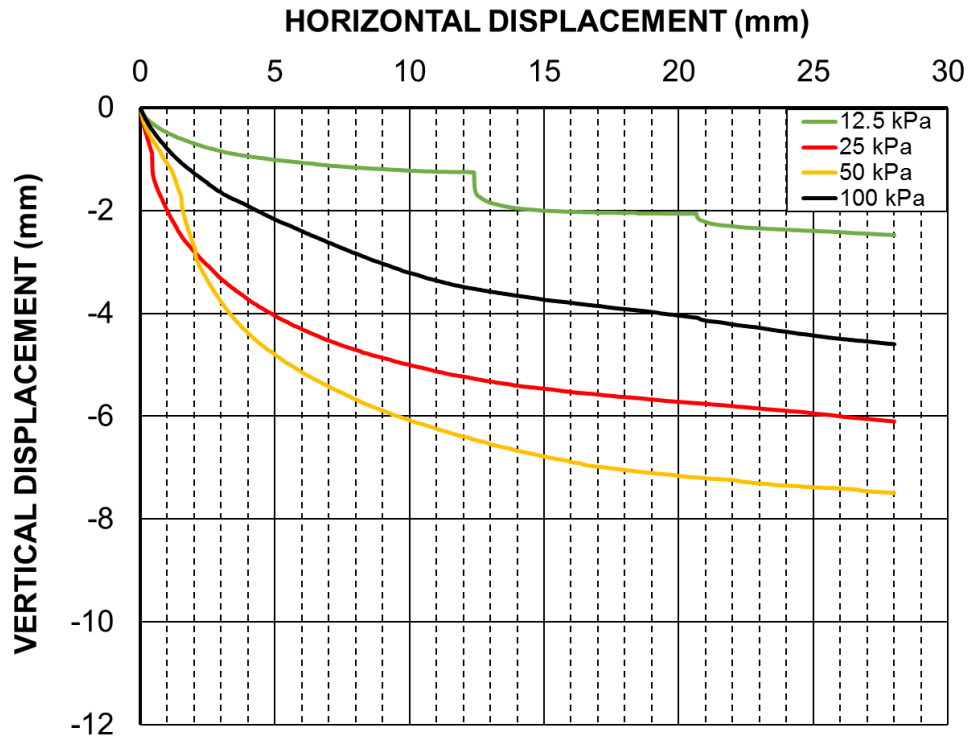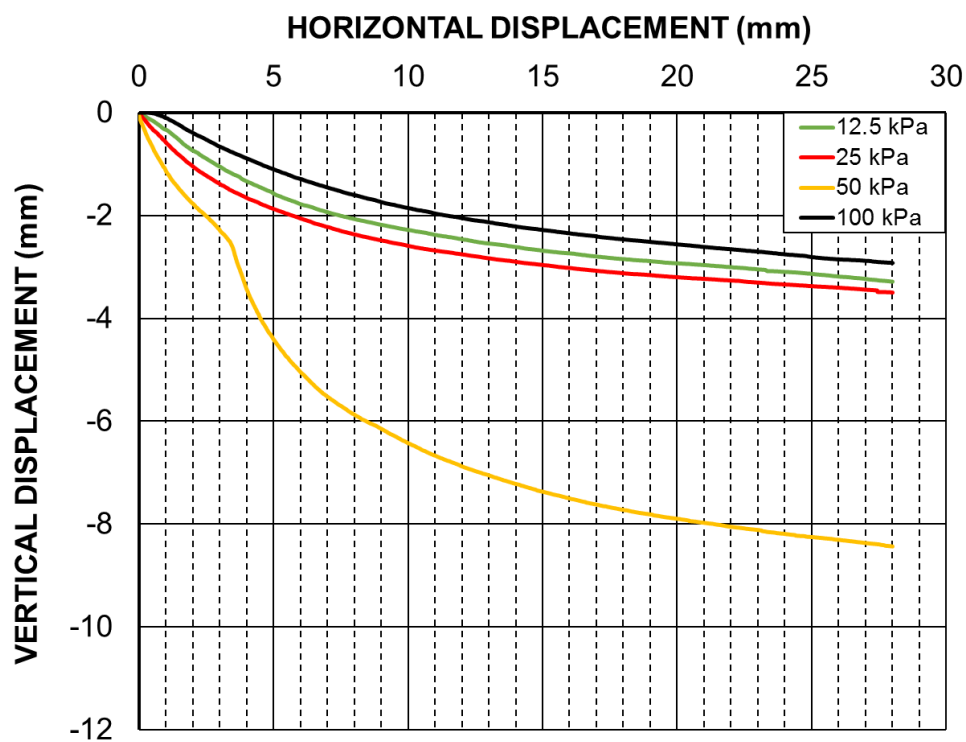

900   **Fig.9c.** Horizontal-vertical stress displacement behaviour of MS-kaolin geocomposite
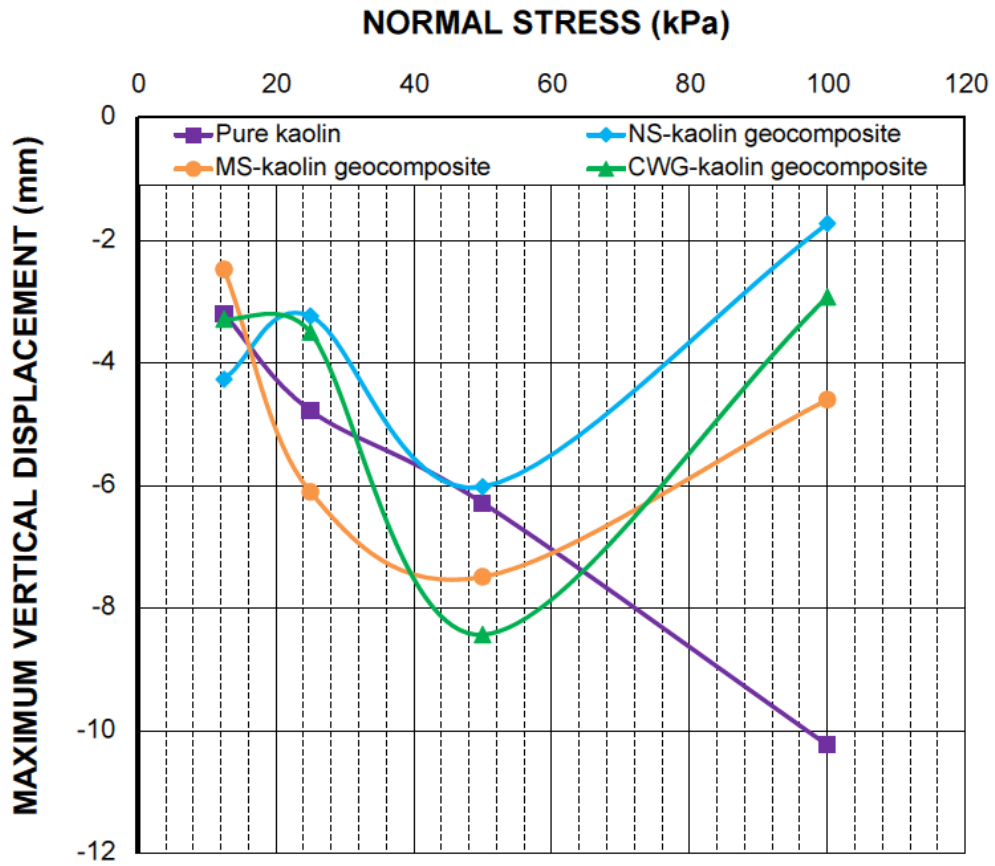
901
902 **Fig.8d.** Shear stress-horizontal displacement behaviour of CWG-kaolin geocomposite

903
904 **Fig.9d.** Horizontal-vertical stress displacement behaviour of CWG-kaolin geocomposite
905

906

907

Fig.10. Maximum vertical displacement-normal stress behaviour of the specimens

Fig.11. Post-shearing cross-section of the geocomposites under 25 kPa normal stress (NS-kaolin, MS-kaolin and CWG-kaolin geocomposite from left to right)